BABAR-CONF-06/16
SLAC-PUB-12012

Updated Measurement of the CKM Angle α Using $B^0 \rightarrow \rho^+\rho^-$ Decays

The *BABAR* Collaboration

July 28, 2006

Abstract

We present results from an analysis of $B^0 \rightarrow \rho^+\rho^-$ using 316 fb^{-1} of $\Upsilon(4S) \rightarrow B\overline{B}$ decays observed with the *BABAR* detector at the PEP-II asymmetric-energy B Factory at SLAC. We measure the $B^0 \rightarrow \rho^+\rho^-$ branching fraction, longitudinal polarization fraction f_L, and the *CP*-violating parameters $S_{\rm long}$ and $C_{\rm long}$:

$$\begin{aligned}
\mathcal{B}(B^0 \rightarrow \rho^+\rho^-) &= (23.5 \pm 2.2(\text{stat}) \pm 4.1(\text{syst}))\times 10^{-6},\\
f_L &= 0.977 \pm 0.024(\text{stat})^{+0.015}_{-0.013}(\text{syst}),\\
S_{\rm long} &= -0.19 \pm 0.21(\text{stat})^{+0.05}_{-0.07}(\text{syst}),\\
C_{\rm long} &= -0.07 \pm 0.15(\text{stat}) \pm 0.06(\text{syst}).
\end{aligned}$$

Using an isospin analysis of $B \rightarrow \rho\rho$ decays we determine the angle α of the unitarity triangle. One of the two solutions, $\alpha = [74, 117]^\circ$ at 68% CL, is compatible with the standard model. All results presented here are preliminary.

Submitted to the 33$^{\rm rd}$ International Conference on High-Energy Physics, ICHEP 06,
26 July—2 August 2006, Moscow, Russia.

Stanford Linear Accelerator Center, Stanford University, Stanford, CA 94309

Work supported in part by Department of Energy contract DE-AC02-76SF00515.

The *BABAR* Collaboration,

B. Aubert, R. Barate, M. Bona, D. Boutigny, F. Couderc, Y. Karyotakis, J. P. Lees, V. Poireau, V. Tisserand, A. Zghiche

Laboratoire de Physique des Particules, IN2P3/CNRS et Université de Savoie, F-74941 Annecy-Le-Vieux, France

E. Grauges

Universitat de Barcelona, Facultat de Fisica, Departament ECM, E-08028 Barcelona, Spain

A. Palano

Università di Bari, Dipartimento di Fisica and INFN, I-70126 Bari, Italy

J. C. Chen, N. D. Qi, G. Rong, P. Wang, Y. S. Zhu

Institute of High Energy Physics, Beijing 100039, China

G. Eigen, I. Ofte, B. Stugu

University of Bergen, Institute of Physics, N-5007 Bergen, Norway

G. S. Abrams, M. Battaglia, D. N. Brown, J. Button-Shafer, R. N. Cahn, E. Charles, M. S. Gill, Y. Groysman, R. G. Jacobsen, J. A. Kadyk, L. T. Kerth, Yu. G. Kolomensky, G. Kukartsev, G. Lynch, L. M. Mir, T. J. Orimoto, M. Pripstein, N. A. Roe, M. T. Ronan, W. A. Wenzel

Lawrence Berkeley National Laboratory and University of California, Berkeley, California 94720, USA

P. del Amo Sanchez, M. Barrett, K. E. Ford, A. J. Hart, T. J. Harrison, C. M. Hawkes, S. E. Morgan, A. T. Watson

University of Birmingham, Birmingham, B15 2TT, United Kingdom

T. Held, H. Koch, B. Lewandowski, M. Pelizaeus, K. Peters, T. Schroeder, M. Steinke

Ruhr Universität Bochum, Institut für Experimentalphysik 1, D-44780 Bochum, Germany

J. T. Boyd, J. P. Burke, W. N. Cottingham, D. Walker

University of Bristol, Bristol BS8 1TL, United Kingdom

D. J. Asgeirsson, T. Cuhadar-Donszelmann, B. G. Fulsom, C. Hearty, N. S. Knecht, T. S. Mattison, J. A. McKenna

University of British Columbia, Vancouver, British Columbia, Canada V6T 1Z1

A. Khan, P. Kyberd, M. Saleem, D. J. Sherwood, L. Teodorescu

Brunel University, Uxbridge, Middlesex UB8 3PH, United Kingdom

V. E. Blinov, A. D. Bukin, V. P. Druzhinin, V. B. Golubev, A. P. Onuchin, S. I. Serednyakov, Yu. I. Skovpen, E. P. Solodov, K. Yu Todyshev

Budker Institute of Nuclear Physics, Novosibirsk 630090, Russia

D. S. Best, M. Bondioli, M. Bruinsma, M. Chao, S. Curry, I. Eschrich, D. Kirkby, A. J. Lankford, P. Lund, M. Mandelkern, R. K. Mommsen, W. Roethel, D. P. Stoker

University of California at Irvine, Irvine, California 92697, USA

S. Abachi, C. Buchanan

University of California at Los Angeles, Los Angeles, California 90024, USA

S. D. Foulkes, J. W. Gary, O. Long, B. C. Shen, K. Wang, L. Zhang
University of California at Riverside, Riverside, California 92521, USA

H. K. Hadavand, E. J. Hill, H. P. Paar, S. Rahatlou, V. Sharma
University of California at San Diego, La Jolla, California 92093, USA

J. W. Berryhill, C. Campagnari, A. Cunha, B. Dahmes, T. M. Hong, D. Kovalskyi, J. D. Richman
University of California at Santa Barbara, Santa Barbara, California 93106, USA

T. W. Beck, A. M. Eisner, C. J. Flacco, C. A. Heusch, J. Kroseberg, W. S. Lockman, G. Nesom, T. Schalk, B. A. Schumm, A. Seiden, P. Spradlin, D. C. Williams, M. G. Wilson
University of California at Santa Cruz, Institute for Particle Physics, Santa Cruz, California 95064, USA

J. Albert, E. Chen, A. Dvoretskii, F. Fang, D. G. Hitlin, I. Narsky, T. Piatenko, F. C. Porter, A. Ryd, A. Samuel
California Institute of Technology, Pasadena, California 91125, USA

G. Mancinelli, B. T. Meadows, K. Mishra, M. D. Sokoloff
University of Cincinnati, Cincinnati, Ohio 45221, USA

F. Blanc, P. C. Bloom, S. Chen, W. T. Ford, J. F. Hirschauer, A. Kreisel, M. Nagel, U. Nauenberg, A. Olivas, W. O. Ruddick, J. G. Smith, K. A. Ulmer, S. R. Wagner, J. Zhang
University of Colorado, Boulder, Colorado 80309, USA

A. Chen, E. A. Eckhart, A. Soffer, W. H. Toki, R. J. Wilson, F. Winklmeier, Q. Zeng
Colorado State University, Fort Collins, Colorado 80523, USA

D. D. Altenburg, E. Feltresi, A. Hauke, H. Jasper, J. Merkel, A. Petzold, B. Spaan
Universität Dortmund, Institut für Physik, D-44221 Dortmund, Germany

T. Brandt, V. Klose, H. M. Lacker, W. F. Mader, R. Nogowski, J. Schubert, K. R. Schubert, R. Schwierz, J. E. Sundermann, A. Volk
Technische Universität Dresden, Institut für Kern- und Teilchenphysik, D-01062 Dresden, Germany

D. Bernard, G. R. Bonneaud, E. Latour, Ch. Thiebaux, M. Verderi
Laboratoire Leprince-Ringuet, CNRS/IN2P3, Ecole Polytechnique, F-91128 Palaiseau, France

P. J. Clark, W. Gradl, F. Muheim, S. Playfer, A. I. Robertson, Y. Xie
University of Edinburgh, Edinburgh EH9 3JZ, United Kingdom

M. Andreotti, D. Bettoni, C. Bozzi, R. Calabrese, G. Cibinetto, E. Luppi, M. Negrini, A. Petrella, L. Piemontese, E. Prencipe
Università di Ferrara, Dipartimento di Fisica and INFN, I-44100 Ferrara, Italy

F. Anulli, R. Baldini-Ferroli, A. Calcaterra, R. de Sangro, G. Finocchiaro, S. Pacetti, P. Patteri, I. M. Peruzzi,[1] M. Piccolo, M. Rama, A. Zallo
Laboratori Nazionali di Frascati dell'INFN, I-00044 Frascati, Italy

[1]Also with Università di Perugia, Dipartimento di Fisica, Perugia, Italy

A. Buzzo, R. Capra, R. Contri, M. Lo Vetere, M. M. Macri, M. R. Monge, S. Passaggio, C. Patrignani, E. Robutti, A. Santroni, S. Tosi

Università di Genova, Dipartimento di Fisica and INFN, I-16146 Genova, Italy

G. Brandenburg, K. S. Chaisanguanthum, M. Morii, J. Wu

Harvard University, Cambridge, Massachusetts 02138, USA

R. S. Dubitzky, J. Marks, S. Schenk, U. Uwer

Universität Heidelberg, Physikalisches Institut, Philosophenweg 12, D-69120 Heidelberg, Germany

D. J. Bard, W. Bhimji, D. A. Bowerman, P. D. Dauncey, U. Egede, R. L. Flack, J. A. Nash, M. B. Nikolich, W. Panduro Vazquez

Imperial College London, London, SW7 2AZ, United Kingdom

P. K. Behera, X. Chai, M. J. Charles, U. Mallik, N. T. Meyer, V. Ziegler

University of Iowa, Iowa City, Iowa 52242, USA

J. Cochran, H. B. Crawley, L. Dong, V. Eyges, W. T. Meyer, S. Prell, E. I. Rosenberg, A. E. Rubin

Iowa State University, Ames, Iowa 50011-3160, USA

A. V. Gritsan

Johns Hopkins University, Baltimore, Maryland 21218, USA

A. G. Denig, M. Fritsch, G. Schott

Universität Karlsruhe, Institut für Experimentelle Kernphysik, D-76021 Karlsruhe, Germany

N. Arnaud, M. Davier, G. Grosdidier, A. Höcker, F. Le Diberder, V. Lepeltier, A. M. Lutz, A. Oyanguren, S. Pruvot, S. Rodier, P. Roudeau, M. H. Schune, A. Stocchi, W. F. Wang, G. Wormser

Laboratoire de l'Accélérateur Linéaire, IN2P3/CNRS et Université Paris-Sud 11, Centre Scientifique d'Orsay, B.P. 34, F-91898 ORSAY Cedex, France

C. H. Cheng, D. J. Lange, D. M. Wright

Lawrence Livermore National Laboratory, Livermore, California 94550, USA

C. A. Chavez, I. J. Forster, J. R. Fry, E. Gabathuler, R. Gamet, K. A. George, D. E. Hutchcroft, D. J. Payne, K. C. Schofield, C. Touramanis

University of Liverpool, Liverpool L69 7ZE, United Kingdom

A. J. Bevan, F. Di Lodovico, W. Menges, R. Sacco

Queen Mary, University of London, E1 4NS, United Kingdom

G. Cowan, H. U. Flaecher, D. A. Hopkins, P. S. Jackson, T. R. McMahon, S. Ricciardi, F. Salvatore, A. C. Wren

University of London, Royal Holloway and Bedford New College, Egham, Surrey TW20 0EX, United Kingdom

D. N. Brown, C. L. Davis

University of Louisville, Louisville, Kentucky 40292, USA

J. Allison, N. R. Barlow, R. J. Barlow, Y. M. Chia, C. L. Edgar, G. D. Lafferty, M. T. Naisbit, J. C. Williams, J. I. Yi

University of Manchester, Manchester M13 9PL, United Kingdom

C. Chen, W. D. Hulsbergen, A. Jawahery, C. K. Lae, D. A. Roberts, G. Simi

University of Maryland, College Park, Maryland 20742, USA

G. Blaylock, C. Dallapiccola, S. S. Hertzbach, X. Li, T. B. Moore, S. Saremi, H. Staengle

University of Massachusetts, Amherst, Massachusetts 01003, USA

R. Cowan, G. Sciolla, S. J. Sekula, M. Spitznagel, F. Taylor, R. K. Yamamoto

Massachusetts Institute of Technology, Laboratory for Nuclear Science, Cambridge, Massachusetts 02139, USA

H. Kim, S. E. Mclachlin, P. M. Patel, S. H. Robertson

McGill University, Montréal, Québec, Canada H3A 2T8

A. Lazzaro, V. Lombardo, F. Palombo

Università di Milano, Dipartimento di Fisica and INFN, I-20133 Milano, Italy

J. M. Bauer, L. Cremaldi, V. Eschenburg, R. Godang, R. Kroeger, D. A. Sanders, D. J. Summers, H. W. Zhao

University of Mississippi, University, Mississippi 38677, USA

S. Brunet, D. Côté, M. Simard, P. Taras, F. B. Viaud

Université de Montréal, Physique des Particules, Montréal, Québec, Canada H3C 3J7

H. Nicholson

Mount Holyoke College, South Hadley, Massachusetts 01075, USA

N. Cavallo,[2] G. De Nardo, F. Fabozzi,[3] C. Gatto, L. Lista, D. Monorchio, P. Paolucci, D. Piccolo, C. Sciacca

Università di Napoli Federico II, Dipartimento di Scienze Fisiche and INFN, I-80126, Napoli, Italy

M. A. Baak, G. Raven, H. L. Snoek

NIKHEF, National Institute for Nuclear Physics and High Energy Physics, NL-1009 DB Amsterdam, The Netherlands

C. P. Jessop, J. M. LoSecco

University of Notre Dame, Notre Dame, Indiana 46556, USA

T. Allmendinger, G. Benelli, L. A. Corwin, K. K. Gan, K. Honscheid, D. Hufnagel, P. D. Jackson, H. Kagan, R. Kass, A. M. Rahimi, J. J. Regensburger, R. Ter-Antonyan, Q. K. Wong

Ohio State University, Columbus, Ohio 43210, USA

N. L. Blount, J. Brau, R. Frey, O. Igonkina, J. A. Kolb, M. Lu, R. Rahmat, N. B. Sinev, D. Strom, J. Strube, E. Torrence

University of Oregon, Eugene, Oregon 97403, USA

[2]Also with Università della Basilicata, Potenza, Italy
[3]Also with Università della Basilicata, Potenza, Italy

A. Gaz, M. Margoni, M. Morandin, A. Pompili, M. Posocco, M. Rotondo, F. Simonetto, R. Stroili, C. Voci

Università di Padova, Dipartimento di Fisica and INFN, I-35131 Padova, Italy

M. Benayoun, H. Briand, J. Chauveau, P. David, L. Del Buono, Ch. de la Vaissière, O. Hamon, B. L. Hartfiel, M. J. J. John, Ph. Leruste, J. Malclès, J. Ocariz, L. Roos, G. Therin

Laboratoire de Physique Nucléaire et de Hautes Energies, IN2P3/CNRS, Université Pierre et Marie Curie-Paris6, Université Denis Diderot-Paris7, F-75252 Paris, France

L. Gladney, J. Panetta

University of Pennsylvania, Philadelphia, Pennsylvania 19104, USA

M. Biasini, R. Covarelli

Università di Perugia, Dipartimento di Fisica and INFN, I-06100 Perugia, Italy

C. Angelini, G. Batignani, S. Bettarini, F. Bucci, G. Calderini, M. Carpinelli, R. Cenci, F. Forti, M. A. Giorgi, A. Lusiani, G. Marchiori, M. A. Mazur, M. Morganti, N. Neri, E. Paoloni, G. Rizzo, J. J. Walsh

Università di Pisa, Dipartimento di Fisica, Scuola Normale Superiore and INFN, I-56127 Pisa, Italy

M. Haire, D. Judd, D. E. Wagoner

Prairie View A&M University, Prairie View, Texas 77446, USA

J. Biesiada, N. Danielson, P. Elmer, Y. P. Lau, C. Lu, J. Olsen, A. J. S. Smith, A. V. Telnov

Princeton University, Princeton, New Jersey 08544, USA

F. Bellini, G. Cavoto, A. D'Orazio, D. del Re, E. Di Marco, R. Faccini, F. Ferrarotto, F. Ferroni, M. Gaspero, L. Li Gioi, M. A. Mazzoni, S. Morganti, G. Piredda, F. Polci, F. Safai Tehrani, C. Voena

Università di Roma La Sapienza, Dipartimento di Fisica and INFN, I-00185 Roma, Italy

M. Ebert, H. Schröder, R. Waldi

Universität Rostock, D-18051 Rostock, Germany

T. Adye, N. De Groot, B. Franek, E. O. Olaiya, F. F. Wilson

Rutherford Appleton Laboratory, Chilton, Didcot, Oxon, OX11 0QX, United Kingdom

R. Aleksan, S. Emery, A. Gaidot, S. F. Ganzhur, G. Hamel de Monchenault, W. Kozanecki, M. Legendre, G. Vasseur, Ch. Yèche, M. Zito

DSM/Dapnia, CEA/Saclay, F-91191 Gif-sur-Yvette, France

X. R. Chen, H. Liu, W. Park, M. V. Purohit, J. R. Wilson

University of South Carolina, Columbia, South Carolina 29208, USA

M. T. Allen, D. Aston, R. Bartoldus, P. Bechtle, N. Berger, R. Claus, J. P. Coleman, M. R. Convery, M. Cristinziani, J. C. Dingfelder, J. Dorfan, G. P. Dubois-Felsmann, D. Dujmic, W. Dunwoodie, R. C. Field, T. Glanzman, S. J. Gowdy, M. T. Graham, P. Grenier,[4] V. Halyo, C. Hast, T. Hryn'ova, W. R. Innes, M. H. Kelsey, P. Kim, D. W. G. S. Leith, S. Li, S. Luitz, V. Luth, H. L. Lynch, D. B. MacFarlane, H. Marsiske, R. Messner, D. R. Muller, C. P. O'Grady, V. E. Ozcan, A. Perazzo, M. Perl, T. Pulliam, B. N. Ratcliff, A. Roodman, A. A. Salnikov, R. H. Schindler, J. Schwiening, A. Snyder, J. Stelzer, D. Su, M. K. Sullivan, K. Suzuki, S. K. Swain, J. M. Thompson, J. Va'vra, N. van

[4]Also at Laboratoire de Physique Corpusculaire, Clermont-Ferrand, France

Bakel, M. Weaver, A. J. R. Weinstein, W. J. Wisniewski, M. Wittgen, D. H. Wright, A. K. Yarritu, K. Yi, C. C. Young

Stanford Linear Accelerator Center, Stanford, California 94309, USA

P. R. Burchat, A. J. Edwards, S. A. Majewski, B. A. Petersen, C. Roat, L. Wilden

Stanford University, Stanford, California 94305-4060, USA

S. Ahmed, M. S. Alam, R. Bula, J. A. Ernst, V. Jain, B. Pan, M. A. Saeed, F. R. Wappler, S. B. Zain

State University of New York, Albany, New York 12222, USA

W. Bugg, M. Krishnamurthy, S. M. Spanier

University of Tennessee, Knoxville, Tennessee 37996, USA

R. Eckmann, J. L. Ritchie, A. Satpathy, C. J. Schilling, R. F. Schwitters

University of Texas at Austin, Austin, Texas 78712, USA

J. M. Izen, X. C. Lou, S. Ye

University of Texas at Dallas, Richardson, Texas 75083, USA

F. Bianchi, F. Gallo, D. Gamba

Università di Torino, Dipartimento di Fisica Sperimentale and INFN, I-10125 Torino, Italy

M. Bomben, L. Bosisio, C. Cartaro, F. Cossutti, G. Della Ricca, S. Dittongo, L. Lanceri, L. Vitale

Università di Trieste, Dipartimento di Fisica and INFN, I-34127 Trieste, Italy

V. Azzolini, N. Lopez-March, F. Martinez-Vidal

IFIC, Universitat de Valencia-CSIC, E-46071 Valencia, Spain

Sw. Banerjee, B. Bhuyan, C. M. Brown, D. Fortin, K. Hamano, R. Kowalewski, I. M. Nugent, J. M. Roney, R. J. Sobie

University of Victoria, Victoria, British Columbia, Canada V8W 3P6

J. J. Back, P. F. Harrison, T. E. Latham, G. B. Mohanty, M. Pappagallo

Department of Physics, University of Warwick, Coventry CV4 7AL, United Kingdom

H. R. Band, X. Chen, B. Cheng, S. Dasu, M. Datta, K. T. Flood, J. J. Hollar, P. E. Kutter, B. Mellado, A. Mihalyi, Y. Pan, M. Pierini, R. Prepost, S. L. Wu, Z. Yu

University of Wisconsin, Madison, Wisconsin 53706, USA

H. Neal

Yale University, New Haven, Connecticut 06511, USA

1 INTRODUCTION

In the standard model, charge conjugation-parity (*CP*) violating effects in the B-meson system arise from a single phase in the Cabibbo-Kobayashi-Maskawa (CKM) quark-mixing matrix [1]. Interference between the direct decay and decay after $B^0\overline{B}^0$ mixing in $B^0 \to \rho^+\rho^-, \rho^\pm\pi^\mp, \pi^+\pi^-$ results in a time-dependent decay-rate asymmetry that is sensitive to the angle $\alpha \equiv \arg\left[-V_{td}V_{tb}^*/V_{ud}V_{ub}^*\right]$ in the unitarity triangle of the CKM matrix. These decays mainly proceed through a $b \to u\overline{u}d$ tree diagram. The presence of penguin loop contributions introduces additional phases that shift the experimentally measurable parameter $\alpha_{\rm eff}$ away from the value of α. Figure 1 shows the leading order tree and gluonic penguin loop contributions to this decay. Measurements of the $B^+ \to \rho^+\rho^0$ [2] and $B^0 \to \rho^0\rho^0$ [3] branching fractions show that the penguin contribution in $B \to \rho\rho$ is smaller than the leading order tree diagram [3]. Results from $B \to \pi\pi$ decays [4, 5] and $B^0 \to \rho^\pm\pi^\mp$ [6, 7] are discussed elsewhere [8].

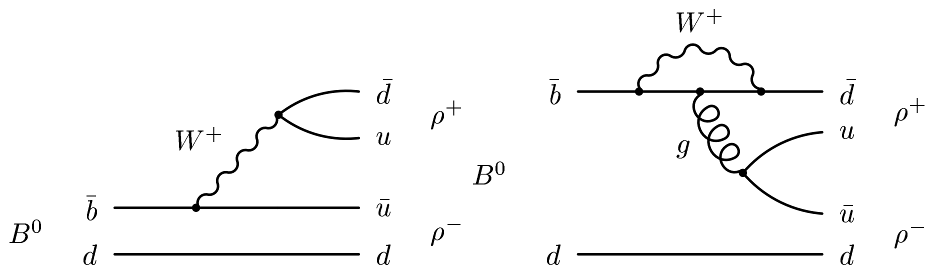

Figure 1: Tree and gluonic penguin diagrams contributing to the process $B^0 \to \rho^+\rho^-$. The penguin contribution coming from the diagram with a top quark in the loop dominates as contributions from processes with u and c quarks are suppressed.

In $B \to \rho\rho$ decays, a spin 0 particle decays into two spin 1 particles (as shown in Fig. 2). Subsequently each ρ meson decays into a $\pi\pi$ pair: $\rho^\pm \to \pi^\pm\pi^0$ and $\rho^0 \to \pi^+\pi^-$. As a result, the *CP* analysis of $B^0 \to \rho^+\rho^-$ is complicated by the presence of one mode with longitudinal polarization and two modes with transverse polarization. The longitudinal mode is *CP* even, while the transverse modes contain *CP*-even and *CP*-odd states. The decay is observed to be dominated by the longitudinal polarization [9], with a fraction f_L defined as the fraction of the helicity zero state in the decay. Integrating over the angle between the ρ decay planes ϕ, the angular decay rate is

$$\frac{d^2\Gamma}{\Gamma d\cos\theta_1 d\cos\theta_2} = \frac{9}{4}\left[f_L \cos^2\theta_1\cos^2\theta_2 + \frac{1}{4}(1-f_L)\sin^2\theta_1\sin^2\theta_2\right], \tag{1}$$

where $\theta_{i=1,2}$ are the angles between the π^0 momentum and the direction opposite to that of the B^0 in the ρ rest frame.

In this paper we present an update of previous *BABAR* measurements of the $B^0 \to \rho^+\rho^-$ branching fraction, longitudinal polarization fraction, *CP*-violating parameters and measurement of the CKM angle α, previously reported in Ref. [9]. There are several theoretical predictions of the branching fraction and f_L in $B^0 \to \rho^+\rho^-$ decays [10]. The branching fraction of $B^0 \to \rho^+\rho^-$ can be used to provide constraints on calculations of the branching fractions and charge asymmetries in $B \to \pi\pi$ and $K\pi$ decays [11].

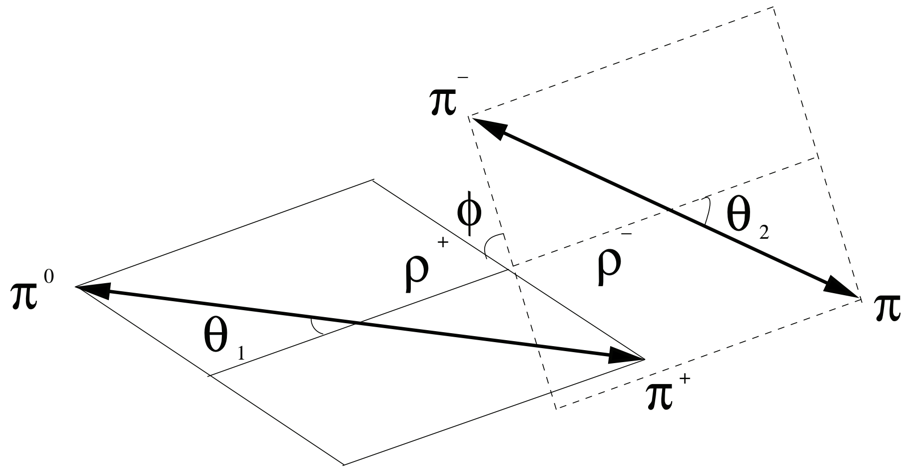

Figure 2: A schematic of the decay of a B meson via two vector particles, ρ^+ and ρ^-, into a four pion final state. The ρ meson final states are shown in their rest frames, and ϕ is the angle between the decay planes of the ρ mesons.

The analysis reported here uses 316 fb^{-1} of data, which is significantly more than our previous branching fraction result (82 fb^{-1}) or f_L and *CP*-violating parameter results (210 fb^{-1}). We have changed the selection requirements in order to reduce background with only a modest reduction in signal efficiency. The new improved probability density-function (PDF) models better account for the correlations between variables entering the maximum likelihood (ML) fit, and result in a reduced systematic uncertainty of the final results.

2 THE *BABAR* DETECTOR AND DATASET

The data used in this analysis were collected with the *BABAR* detector at the PEP-II asymmetric-energy B Factory at SLAC. This represents a total integrated luminosity of 316 fb^{-1} taken at the $\Upsilon(4S)$ resonance (on-peak), corresponding to a sample of $(347 \pm 3.9) \times 10^6$ $B\overline{B}$ pairs. An additional 27.2 fb^{-1} of data, collected at approximately 40 MeV below the $\Upsilon(4S)$ resonance (off-peak), were used to study background from non-resonant (continuum) $e^+e^- \rightarrow q\overline{q}$ events, where $q = u, d, s, c$.

The detector is described in detail elsewhere [12]. Surrounding the interaction point is a five double-sided layer silicon vertex tracker (SVT) which measures the impact parameters of charged particle tracks in both the plane transverse to, and along the beam direction. A 40 layer drift chamber (DCH) surrounds the SVT and provides measurements of the momenta for charged particles. Both the SVT and the DCH operate in the magnetic field of a 1.5 T solenoid. Charged hadron identification is achieved through measurements of particle energy-loss in the tracking system and the Cherenkov angle obtained from a detector of internally reflected Cherenkov light. A CsI(Tl) electromagnetic calorimeter provides photon detection, electron identification, and π^0 reconstruction. Finally, the instrumented flux return of the magnet allows discrimination of muons from pions. We use the GEANT4 [13] software to simulate interactions of particles traversing the *BABAR* detector.

3 EVENT SELECTION

We reconstruct $B^0 \to \rho^+\rho^-$ candidates (B_{rec}) from combinations of two charged tracks and two π^0 candidates. We require that both tracks have particle identification information inconsistent with the electron, kaon, and proton hypotheses. The π^0 candidates are formed from pairs of photons, each of which has a measured energy greater than 50 MeV. The reconstructed π^0 mass must satisfy $0.10 < m_{\gamma\gamma} < 0.16$ GeV/c^2. The mass of the ρ candidates must satisfy $0.5 < m_{\pi^\pm\pi^0} < 1.0$ GeV/c^2.

Continuum events are the dominant background which is reduced by requiring that $|\cos(TB, TR)|$ be less than 0.8, where $|\cos(TB, TR)|$ is the absolute value of the cosine of the angle between the B_{rec} thrust axis and that of the rest of the event (ROE) calculated in the CM frame. To distinguish signal from continuum we use a neural network ($\mathcal{N}$) combining the following eight discriminating variables.

- The coefficients, L_0, L_2, where these are split into sums over the ROE for neutral and charged particles. The coefficients are defined as:

$$L_0 = \sum_{ROE} p_j \tag{2}$$

$$L_2 = \sum_{ROE} p_j |\cos(\psi_j)|^2 \tag{3}$$

  where p_j is the particle momentum and ψ_j is the angle of the particle direction relative to the thrust axis of the B candidate in the center-of-mass (CM) frame.

- $|\cos(B, Z)|$, the absolute value of the cosine of the angle between the direction of the B and z axis in the CM frame, where the z axis is along the electron beam direction.

- $|\cos(TB, TR)|$ as previously defined.

- $|\cos(TB, Z)|$, the absolute value of the cosine of the angle between the B thrust and the z axis.

- the sum of the transverse momentum p_t of the ROE relative to the z axis.

Continuum backgrounds dominate near $|\cos\theta_i| = 1$, and backgrounds from B decays tend to concentrate at negative values of $\cos\theta_i$. We reduce these backgrounds with the requirement $-0.90 < \cos\theta_i < 0.98$.

Signal events are identified kinematically using two variables, the difference ΔE between the CM energy of the B candidate E_B and $\sqrt{s}/2$

$$\Delta E = E_B - \sqrt{s}/2, \tag{4}$$

and the beam-energy-substituted mass

$$m_{ES} = \sqrt{(s/2 + \mathbf{p}_i \cdot \mathbf{p}_B)^2 / E_i^2 - \mathbf{p}_B^2}, \tag{5}$$

where $\sqrt{s}$ is the total CM energy. The B momentum $\mathbf{p}_B$ and four-momentum of the initial state $(E_i, \mathbf{p}_i)$ are measured in the laboratory frame. We accept candidates that satisfy $5.25 < m_{ES} < 5.29$ GeV/c^2 and $-0.12 < \Delta E < 0.15$ GeV. An asymmetric ΔE selection is used in order to reduce background from higher-multiplicity B decays.

When multiple B candidates are formed, we select the one that minimizes the sum of $(m_{\gamma\gamma} - m_{\pi^0})^2$ where m_{π^0} is the π^0 mass reported in [14]. In 0.3% the same π^0 mesons are used by multiple B candiadtes. We randomly select the candidate entering the fit for such events.

In order to study the time-dependent decay-rate asymmetry one needs to measure the proper-time difference Δt between the two B decays in the event, and to determine the flavor of the other B meson ($B_{\rm tag}$). We calculate Δt from the measured separation Δz between the $B_{\rm rec}$ and $B_{\rm tag}$ decay vertices [15]. We determine the $B_{\rm rec}$ vertex from the two charged-pion tracks in its decay. The $B_{\rm tag}$ decay vertex is obtained by fitting the other tracks in the event, with constraints from the $B_{\rm rec}$ momentum and the beam-spot location. The RMS resolution on Δt is 1.1 ps. We only use events that satisfy $|\Delta t| < 15$ ps and have an error on Δt of less than 2.5 ps. The flavor of the $B_{\rm tag}$ meson is determined with a multivariate technique [16]. The performance of this algorithm is summarised in Table 1 for the seven mutually-exclusive tag categories. Events are categorised according to decreasing signal purity and increasing mistag probability ω. The categories assigned correspond to events with leptons, kaons and pions in the decay products of $B_{\rm tag}$. The `Untagged` category of events are dominated by continuum background, have a mistag probability of 50%, and are not used in this analysis.

Table 1: Tagging efficiency ϵ_c, average mistag fraction ω_c, and mistag fraction difference $\Delta\omega_c$ between B^0 and $\overline{B}^0$ tagged events for $B^0 \to \rho^+\rho^-$ events in each tagging category.

Category (c)	ϵ_c	ω_c	$\Delta\omega_c$
`Lepton`	0.080 ± 0.001	0.032 ± 0.004	0.002 ± 0.008
`Kaon 1`	0.114 ± 0.001	0.053 ± 0.005	-0.012 ± 0.009
`Kaon 2`	0.176 ± 0.002	0.152 ± 0.005	-0.015 ± 0.008
`Kaon-Pion`	0.135 ± 0.002	0.233 ± 0.006	-0.018 ± 0.010
`Pion`	0.137 ± 0.002	0.327 ± 0.007	0.059 ± 0.010
`Other`	0.095 ± 0.001	0.412 ± 0.008	0.042 ± 0.001
`Untagged`	0.266 ± 0.002	0.500 ± 0.000	0.000 ± 0.000

Mis-reconstructed signal candidates or self-cross-feed (SCF) signal may pass the selection requirements even if one or more of the pions assigned to the $\rho^+\rho^-$ state belongs to the other B in the event. These SCF candidates constitute 50.7% (27.9%) of the accepted longitudinally (transversely) polarised signal. The majority of SCF events have both charged pions from the $\rho^+\rho^-$ final state, and unbiased *CP* information. These correct track SCF events are denoted by CT SCF. There is a SCF component (13.8% of the signal) where at least one track in $B_{\rm rec}$ is from the ROE. These wrong track (WT) events have biased *CP* information, and are treated separately for the *CP* result. The PDF describing WT events is used only to determine the signal yield and polarization. A systematic error is assigned to the *CP* results from this type of signal event. The total selection efficiency for longitudinally (transversely) polarised signal is 7.7% (10.5%).

4 MAXIMUM LIKELIHOOD FIT

We obtain a sample of 33902 events that enter an unbinned extended ML fit. These events are dominated by backgrounds from $q\overline{q}$ (81.4%) and $B\overline{B}$ (16.6%) events. The remaining 2% of events are signal. We distinguish between the following components in the fit: (i) correctly reconstructed signal; (ii) SCF signal, split into CT and WT parts; (iii) charm $B^{\pm}$ background ($b \to c$); (iv) charm B^0 background ($b \to c$); (v) charmless B^0 backgrounds; (vi) charmless $B^{\pm}$ backgrounds; and (vii) continuum background. The dominant B backgrounds come from categories (iii) and (iv). The dominant charmless backgrounds are summarised in Table 2. The branching fractions of $B^{\pm} \to (a_1\pi)^{\pm}$ decays have been estimated using the measurements of $B^0 \to a_1^{\pm}\pi^{\mp}$ [17].

Table 2: Dominant charmless backgrounds with assumed or measured branching fraction and the number of selected events in the data sample.

Decay	Branching fraction (10^{-6})	Number of events
$a_1^{\pm}\pi^{\mp}$	39.7 ± 3.7 [17]	94 ± 9
$\rho^0\rho^+$ (long)	19.1 ± 3.5 [2]	70 ± 13
$a_1^+\pi^0$	20 ± 20	55 ± 55
$a_1^0\pi^+$	20 ± 20	45 ± 45
$a_1^{\pm}\rho^{\mp}$ (long)	24 ± 2.5 [18]	40 ± 4
$\rho^{\pm}\pi^{\mp}$	30 ± 30 [19]	40 ± 40

We allow the charm and the non-resonant $B^0 \to \rho^+\pi^-\pi^0$ yields to vary in the fit to data. The remaining background yields are fixed to their expected values determined from measured branching fractions where available [20].

The likelihood function incorporates the following previously defined eight variables to distinguish signal from background: m_{ES}, ΔE, Δt, $\mathcal{N}$, and the $m_{\pi^{\pm}\pi^0}$, and $\cos\theta_i$ values of the two ρ mesons. For each of the aforementioned components we construct a PDF that is the product of one-dimensional PDFs for each of the variables. The PDFs for all of the components are combined to give the likelihood function used in the fit. Table 3 summarises the PDF shapes used for different components of the signal.

The B background ΔE distributions are described by 3^{rd} order polynomials, except for non-resonant $B^0 \to \rho^+\pi^-\pi^0$ which uses a non-parametric (NP) PDF. The m_ρ distributions for true ρ mesons are parametersised using a relativistic Breit-Wigner, and the fake m_ρ (combinatorial $\pi^{\pm}\pi^0$) distribution is described using 3^{rd} order polynomials. The m_{ES} distribution of $b \to c$ backgrounds is described using a phase-space-motivated distribution [21]. All remaining background shapes are described using NP PDFs.

The continuum distribution for m_{ES} is described by a phase-space-motivated distribution [21]. The ΔE and $\mathcal{N}$ shapes are modeled with 3^{rd} and 4^{th} order polynomials, respectively. The parameters of the m_{ES}, ΔE and $\mathcal{N}$ shapes are allowed to vary in the fit to data. The continuum $m_{\pi^{\pm}\pi^0}$ distribution is described using a relativistic Breit-Wigner and a 3^{rd} order polynomial PDF for true and fake ρ contributions, respectively. The $\cos\theta_i$ distribution is described by a 3^{rd} order polynomial. The parameters of the $m_{\pi^{\pm}\pi^0}$ and $\cos\theta_i$ distributions are obtained from a fit to the off-peak data.

The signal decay-rate distribution for both polarizations $f_+(f_-)$ for B_{tag}= B^0 ($\overline{B}^0$) is given by

$$f_{\pm}(\Delta t) = \frac{e^{-|\Delta t|/\tau}}{4\tau}[1 \pm S\sin(\Delta m_d\Delta t) \mp C\cos(\Delta m_d\Delta t)] \tag{6}$$

where τ is the mean B^0 lifetime, Δm_d is the $B^0\overline{B}^0$ mixing frequency, and $S = S_{\text{long}}$ or S_{tran} and $C = C_{\text{long}}$ or C_{tran} are the CP-asymmetry parameters for the longitudinally and transversely polarized

Table 3: PDFs used to parameterize signal distributions. The abbreviations used are as follows: long− *longitudinal signal Monte Carlo (MC) simulated data*; tran− *transverse signal MC simulated data*; true− *true signal (or in the case of background, true ρ meson)*; SCF− *SCF signal*; pN − *polynomial of order N*; G − *a Gaussian distribution*; CB − *a Gaussian with an exponential tail which takes the form of [22]*; NP − *a non-parametric PDF defined as smoothed histogram of MC simulated data*; RBW − *a relativistic Breit-Wigner*; SigDT − *a distribution of the form of Eq. 6, convoluted with a triple Gaussian resolution function.* Where indicated, the PDF denoted by pN acc. refers to the physical distribution multiplied by a polynomial acceptance function of order N.

Component	m_{ES}	ΔE	$\mathcal{N}$	Δt	$\cos\theta_\rho$		m_ρ	
					True	Fake	True	Fake
true (long)	CB	CB+G	NP	SigDT	p4 acc.	N.A.	RBW	N.A.
true (tran)	CB+G	CB+G	NP	SigDT	p4 acc.	N.A.	RBW	N.A.
CT SCF(long) (TT)	CB	p2+G	NP	SigDT	p6 acc.	NP	RBW	p3
CT SCF(long) (TF/FT)	CB+G	p2	NP	SigDT	p6 acc.	NP	RBW	p3
CT SCF(long) (FF)	CB+G	p1	NP	SigDT	p6 acc.	NP	RBW	p3
WT SCF(long) (TF/FT)	CB+G	p2	NP	SigDT	p6 acc.	NP	RBW	p3
WT SCF(long) (FF)	CB+G	p1	NP	SigDT	p6 acc.	NP	RBW	p3
SCF(tran)	CB+G	GG	NP	SigDT	NP	NP	NP	NP

signal. The parameters S and C describe B-mixing induced and direct CP violation, respectively. S and C for the longitudinally polarized WT signal are set to zero. The Δt PDF takes into account incorrect tags and is convolved with the resolution function described below. Since f_L is approximately 1, the fit has no sensitivity to either S_{tran} or C_{tran}. We set these parameters to zero and we vary them in the evaluation of systematic uncertainties.

The signal Δt resolution function consists of three Gaussians ($\sim 85\%$ core, $\sim 14\%$ tail, $\sim 1\%$ outliers), and takes into account the per-event error on Δt from the vertex fit. The resolution function parameters are obtained from a large sample of fully reconstructed hadronic B decays [15]. For WT SCF we replace the B-meson lifetime by an effective lifetime obtained from Monte Carlo (MC) simulation to account for the difference in the resolution. The nominal Δt distribution for the B backgrounds is a NP PDF representation of the MC samples; in the study of systematic errors we replace this model with the one used for signal. The resolution for continuum background is described by the sum of three Gaussian distributions whose parameters are determined from data.

5 RESULTS

From the extended maximum likelihood fit described above, we obtain the following results

$$\begin{aligned} N(\text{signal}) &= 615 \pm 57(\text{stat}), \\ f_L &= 0.977 \pm 0.024(\text{stat}), \\ S_{\text{long}} &= -0.19 \pm 0.21(\text{stat}), \\ C_{\text{long}} &= -0.07 \pm 0.15(\text{stat}), \end{aligned}$$

after correction for a +28 event fit bias on the signal yield and a correction for a −0.007 fit bias on f_L. We discuss the origin of these fit biases in Section 6. The $B^0 \to \rho^\pm\pi^\mp\pi^0$ background yield obtained from the fit is 9.2 ± 53.6 events. Figure 3 shows distributions of m_{ES}, ΔE, $\cos\theta_i$ and $m_{\pi^\pm\pi^0}$ for the highest purity tagged events with a loose requirement on $\mathcal{N}$. The plot of m_{ES} contains 15.6% of the signal and 1.1% of the background. For the other plots there is an added constraint that $m_{ES} > 5.27\,\mathrm{GeV}/c^2$; these requirements retain 13.9% of the signal and 0.4% of the background. Figure 4 shows the Δt distribution for B^0 and $\overline{B}^0$ tagged events. The time-dependent decay-rate asymmetry

$$a_{CP}(\Delta t) = \frac{N(\Delta t) - \overline{N}(\Delta t)}{N(\Delta t) + \overline{N}(\Delta t)} \tag{7}$$

is also shown, where N ($\overline{N}$) is the decay-rate for B^0 ($\overline{B}^0$) tagged events.

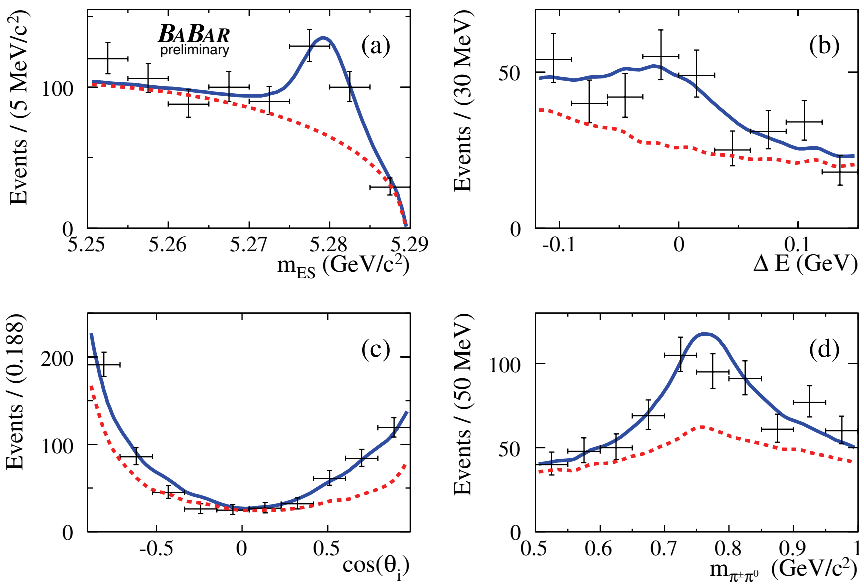

Figure 3: The distributions for the highest purity tagged events for the variables m_{ES} (a), ΔE (b), cosine of the ρ helicity angle (c) and $m_{\pi^\pm\pi^0}$ (d). The dashed lines are the sum of backgrounds, and the solid lines are the full PDF.

6 SYSTEMATIC ERROR STUDIES

Table 4 lists the possible sources of systematic uncertainties on the values of the signal yield, f_L, S_{long} and C_{long} that have been studied. The systematic uncertainties, listed in Table 4, are briefly discussed in the following.

- The uncertainty from PDF parameterisation is obtained by varying PDF shape parameters by $\pm 1\sigma$, in turn. The deviations obtained are added in quadrature to give the quoted uncertainty from the PDF parameterisation.
- The systematic uncertainty on the yield from the fraction of SCF events is obtained taking the difference between the nominal result and the number of events fitted (after correcting for the fraction of SCF events in MC simulated data) when using the true signal PDFs to extract

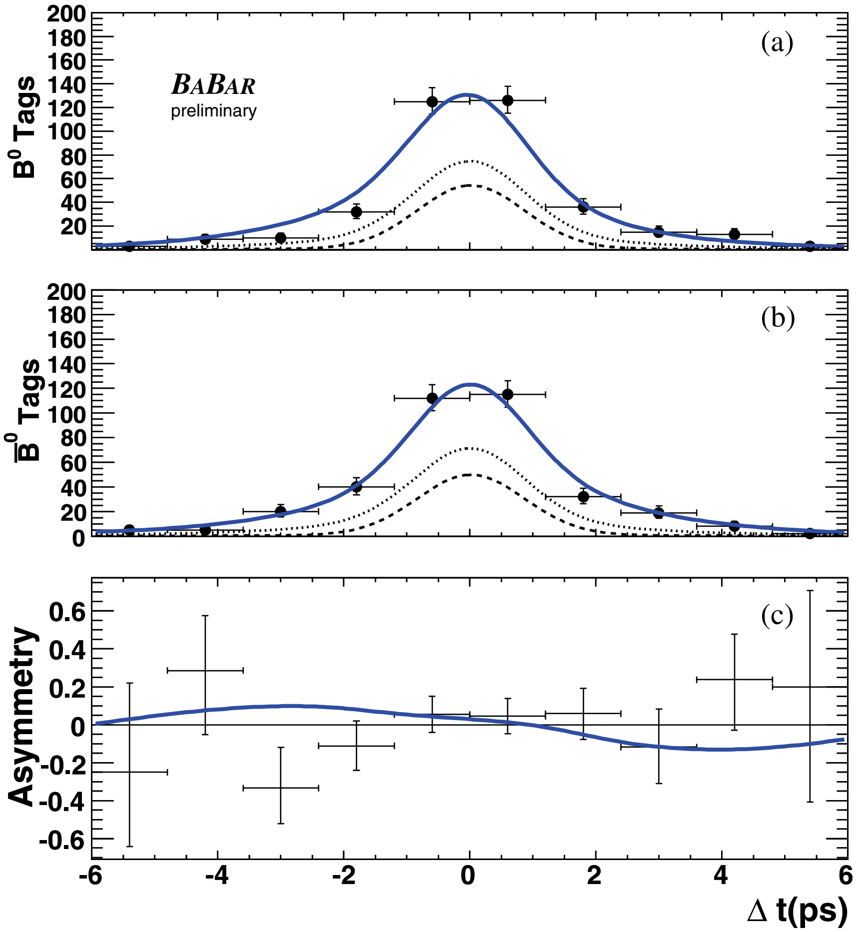

Figure 4: The Δt distribution for a sample of events enriched in signal for (a) B^0 and (b) $\overline{B}^0$ tagged events. The dotted lines are the sum of backgrounds, the dashed lines are the $q\overline{q}$ background and the solid lines are the sum of signal and backgrounds. The time-dependent CP asymmetry (see text) is shown in (c), where the curve is the measured asymmetry.

the yield. The uncertainty on the other signal observables comes from varying the fraction of SCF events by 5% per π^0 (10% total), which is twice the observed data/MC difference seen in our control sample of $B^0 \to D^- \rho^+$ events.

- The uncertainty on the m_{ES} and ΔE widths is obtained from the observed shifts relative to our nominal result, when allowing these parameters to vary independently in the fit to data.

- We vary the B background normalisation within expectations for each background in turn. The deviations obtained when doing this are added in quadrature to give the quoted uncertainty from this source.

- As the branching fractions of some of the B backgrounds are not well known, we assign an additional uncertainty coming from the maximum shifts obtained when allowing each of the fixed backgrounds to vary in turn in the fit to data.

- Additional uncertainties on the *CP* results come from possible *CP* violation in the B background. We use existing experimental constraints where possible, otherwise we allow for a *CP* asymmetry up to 10% in B decays to final states with charm, and up to 50% in B decays to charmless final states.

- The physics parameters $\tau = 1.530 \pm 0.009$ ps and $\Delta m_d = 0.507 \pm 0.005\ \hbar\,\mathrm{ps}$ [14] are varied within the quoted uncertainty.

- The tagging and mistag fractions for signal and the B backgrounds are corrected for data/MC differences observed in samples of fully reconstructed hadronic B decays. Each of the tagging and mistag parameters is varied in turn by the uncertainty from the correction. The deviations obtained when doing this are added in quadrature to give the quoted uncertainty from this source.

- Allowing for possible *CP* violation in the transverse polarization, and in the WT longitudinally polarised signal SCF events results in additional uncertainties on signal observables. We vary S and C by ± 0.5 (± 1.0) for the transverse polarisation (WT SCF).

- Possible *CP* violation from interference in doubly Cabibbo-suppressed decays (DCSD) on the tag side of the event [23] contribute to systematic uncertainties on S_{long} and C_{long}.

- We estimate the systematic error on our results coming from neglecting the interference between $B^0 \rightarrow \rho^+\rho^-$ and other 4π final states: $B \rightarrow a_1\pi$, $\rho\pi\pi^0$ and $B \rightarrow \pi\pi\pi^0\pi^0$. Strong phases are varied between -180 and 180 degrees, and the *CP* content of the interfering amplitudes are varied between zero and maximum using uniform prior distributions, and the RMS deviation of the parameters from nominal is taken as the systematic error. We assume that the amplitudes for $B \rightarrow \rho\pi\pi^0$ and $\pi\pi\pi^0\pi^0$ are equal to the amplitude of $B \rightarrow a_1\pi$ when calculating this systematic uncertainty.

- As the PDFs used in the ML fit do not account for all of the correlations between discriminating variables used in the fit, the results have a small bias. We calculate the fit bias on the signal observables from ensembles of experiments obtained from samples of signal and charmless B background MC simulated events combined with charm and $q\overline{q}$ background events simulated from the PDFs. The 28 event bias on signal yield and 0.007 bias on f_L is corrected, and 100% of the calculated fit bias is assigned as a systematic uncertainty on all signal observables. We do not observe a significant bias on S_{long} and C_{long}.

- Small imperfections in the knowledge of the geometry of the SVT over time can affect the measurement of S_{long} and C_{long}. We vary the alignment according to the results obtained from the study of $e^+e^- \rightarrow e^+e^-, \mu^+\mu^-$ events in order to estimate the magnitude of this systematic error on our *CP* results.

The branching fraction has multiplicative systematic uncertainties from the reconstruction of π^0 mesons in the detector (6%), uncertainties in the reconstruction of charged particles (0.8%), and the discrimination of $\pi^\pm$ from other types of charged particles (1%). In addition to these uncertainties, there is a 1.1% uncertainty on the number of $B\overline{B}$ pairs in the data sample. Statistical uncertainties arising from the MC samples used in this analysis are negligible.

Table 4: Summary of additive systematic uncertainty contributions.

Contribution	$\sigma(N_{signal})$	$\sigma(f_L)$	$\sigma(S_{\text{long}})$	$\sigma(C_{\text{long}})$
PDF parameterisation	$^{+16.7}_{-30.2}$	$^{+0.0082}_{-0.0064}$	$^{+0.0149}_{-0.0425}$	$^{+0.0300}_{-0.0306}$
SCF fraction	84.0	$^{+0.0007}_{-0.0011}$	$^{+0.00235}_{-0.00355}$	$^{+0.0070}_{-0.00683}$
m_{ES} and ΔE width	22.9	0.005	0.011	0.012
B background normalisation	$^{+16.0}_{-17.2}$	$^{+0.0033}_{-0.0038}$	$^{+0.0096}_{-0.0115}$	$^{+0.0024}_{-0.0015}$
floating B backgrounds	33.6	0.004	0.033	0.006
CPV in B background	$^{+3.3}_{-2.0}$	$^{+0.0006}_{-0.0016}$	$^{+0.0059}_{-0.0214}$	$^{+0.0118}_{-0.0115}$
τ	$^{+0.1}_{-0.4}$	$^{+0.0000}_{-0.0002}$	$^{+0.0002}_{-0.0008}$	0.0007
Δm	$^{+0.0}_{-0.2}$	$^{+0.0000}_{-0.0002}$	$^{+0.0014}_{-0.0020}$	$^{+0.0018}_{-0.0012}$
tagging and dilution	$^{+2.6}_{-8.1}$	$^{+0.0029}_{-0.0021}$	$^{+0.0016}_{-0.0053}$	$^{+0.0068}_{-0.0054}$
transverse polarisation CPV	$^{+0.0}_{-8.3}$	$^{+0.0057}_{-0.0000}$	$^{+0.0125}_{-0.0152}$	$^{+0.0095}_{-0.0110}$
WT SCF CPV	$^{+0.2}_{-1.1}$	$^{+0.0000}_{-0.0003}$	$^{+0.0051}_{-0.0065}$	$^{+0.0116}_{-0.0113}$
DCSD decays	–	–	0.012	0.037
Interference	14.8	0.0036	0.023	0.022
Fit Bias	28	0.007	0.002	0.022
SVT Alignment	–	–	0.0100	0.0055
Total	$^{+97}_{-101}$	$^{+0.015}_{-0.013}$	$^{+0.05}_{-0.07}$	± 0.06

7 FINAL RESULTS

Our results are

$$\begin{aligned}
\mathcal{B}(B^0 \to \rho^+\rho^-) &= (23.5 \pm 2.2(\text{stat}) \pm 4.1(\text{syst}))\times 10^{-6},\\
f_L &= 0.977 \pm 0.024(\text{stat})^{+0.015}_{-0.013}(\text{syst}),\\
S_{\text{long}} &= -0.19 \pm 0.21(\text{stat})^{+0.05}_{-0.07}(\text{syst}),\\
C_{\text{long}} &= -0.07 \pm 0.15(\text{stat}) \pm 0.06(\text{syst}).
\end{aligned}$$

where the correlation between S_{long} and C_{long} is -0.058. This measurement corresponds to $\alpha_{\text{eff}} = (95.5^{+6.9}_{-6.2})^{\circ}$, where $S_{\text{long}} = \sqrt{1 - C^2_{\text{long}}}\sin 2\alpha^{\rho\rho}_{eff}$. The measured branching fraction, polarization, and *CP* parameters are in agreement with our earlier publication [9], with significantly improved precision.

We constrain the CKM angle α from an isospin analysis [24] of $B \to \rho\rho$. The inputs to the isospin analysis are the amplitudes of the *CP*-even longitudinal polarization of the $\rho\rho$ final state, as well as the measured values of S_{long} and C_{long} for $B^0 \to \rho^+\rho^-$. We use the following numerical inputs in the isospin analysis:

- The average of the measurements of $\mathcal{B}(B^0 \to \rho^+\rho^-)$ and f_L, presented here, and those reported in Ref. [25].
- The combined branching fraction and f_L for $B \to \rho^+\rho^0$ from Ref. [2].
- The central value corresponding to the upper limit of $\mathcal{B}(B \to \rho^0\rho^0)$ from Ref. [3].
- S_{long} and C_{long} presented here.

We ignore possible $I = 1$ amplitudes [26] and electroweak penguins in this paper.

To interpret our results in terms of a constraint on α from the isospin relations, we construct a χ^2 that includes the measured quantities expressed as the lengths of the sides of the isospin triangles and we determine the minimum χ^2_0. We have adopted a simulated experiment technique to compute the confidence level (CL) on α; our method is similar to the approach proposed in Ref. [27]. For each value of α, scanned between 0 and 180°, we determine the difference $\Delta\chi^2_{\text{DATA}}(\alpha)$ between the minimum of $\chi^2(\alpha)$ and χ^2_0. We then generate MC experiments around the central values obtained from the fit to data with the given value of α and we apply the same procedure. The fraction of these experiments in which $\Delta\chi^2_{\text{MC}}(\alpha)$ is smaller than $\Delta\chi^2_{\text{DATA}}(\alpha)$ is interpreted as the CL on α. Figure 5 shows $1 - \text{CL}$ for α obtained from this method. Selecting the solution closest to the CKM combined fit average [28, 29] we find $\alpha = [74, 117]^{\circ}$ at 68% CL, where the error is dominated by $|\alpha_{\text{eff}} - \alpha|$ which is 18° at 68% CL. The constraint obtained on α is less precise than the previous result in Ref. [9] for the following reasons: (i) the improved world average branching fraction for $B^+ \to \rho^+\rho^0$ has come down, and (ii) the results of the latest search for $B^0 \to \rho^0\rho^0$ show evidence for a signal. Both of these factors lead to an increase in the the penguin contribution to the total uncertainty on α when using an isospin analysis.

It is possible to calculate a model-dependent constraint on α using $SU(3)$ as detailed in Ref. [30]. This model relates the penguin amplitude in $B^+ \to K^{*0}\rho^+$ to the penguin amplitude in $B^0 \to \rho^+\rho^-$, and can be used to obtain a more precise, but model dependent constraint on α.

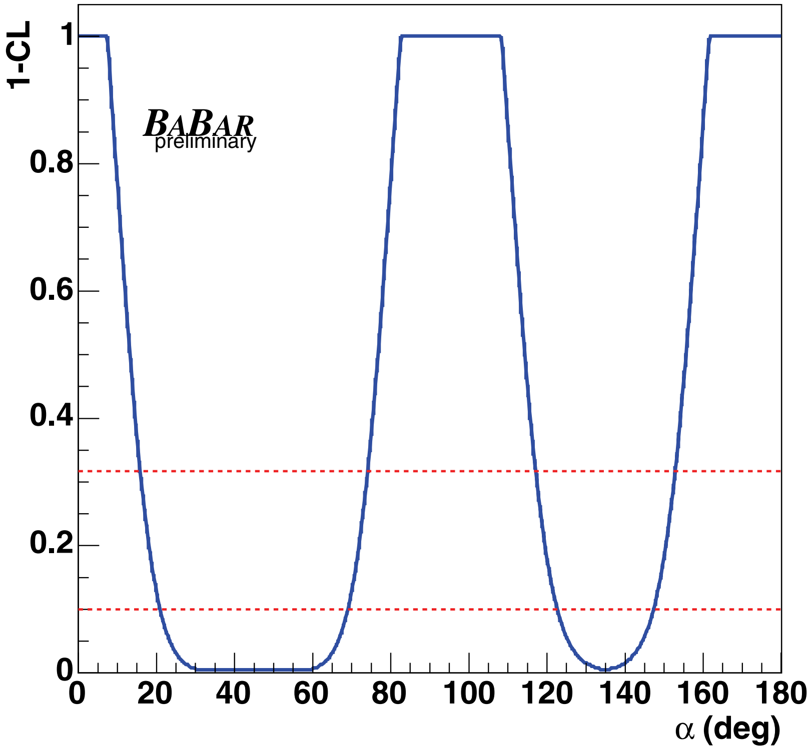

Figure 5: Confidence level on α obtained from the isospin analysis with the statistical method described in [28]. The dashed lines correspond to the 68% (top) and 90% (bottom) CL intervals.

8 SUMMARY

In summary we have improved the measurement of the branching fraction, f_L, and *CP*-violating parameters $S_{\rm long}$ and $C_{\rm long}$ in $B^0 \to \rho^+\rho^-$ using a data-sample of $(347 \pm 3.9) \times 10^6$ $B\overline{B}$ pairs. We do not observe mixing-induced or direct *CP* violation. We derive a model-independent measurement of the CKM angle α. The results presented in this paper are consistent with previous results presented by *BABAR* [9] and Belle [25].

9 ACKNOWLEDGMENTS

We are grateful for the extraordinary contributions of our PEP-II colleagues in achieving the excellent luminosity and machine conditions that have made this work possible. The success of this project also relies critically on the expertise and dedication of the computing organizations that support *BABAR*. The collaborating institutions wish to thank SLAC for its support and the kind hospitality extended to them. This work is supported by the US Department of Energy and National Science Foundation, the Natural Sciences and Engineering Research Council (Canada), Institute of High Energy Physics (China), the Commissariat à l'Energie Atomique and Institut National de Physique Nucléaire et de Physique des Particules (France), the Bundesministerium für

Bildung und Forschung and Deutsche Forschungsgemeinschaft (Germany), the Istituto Nazionale di Fisica Nucleare (Italy), the Foundation for Fundamental Research on Matter (The Netherlands), the Research Council of Norway, the Ministry of Science and Technology of the Russian Federation, and the Particle Physics and Astronomy Research Council (United Kingdom). Individuals have received support from the Marie-Curie IEF program (European Union) and the A. P. Sloan Foundation.

References

[1] N. Cabibbo, Phys. Rev. Lett. **10**, 531 (1963);
M. Kobayashi and T. Maskawa, Prog. Theor. Phys. **49**, 652 (1973).

[2] *BABAR* Collaboration, B. Aubert *et al.*, hep-ex/0607095;
Belle Collaboration, J. Zhang *et al.*, Phys. Rev. Lett. **91**, 221801 (2003).

[3] *BABAR* Collaboration, B. Aubert *et al.*, BABAR-CONF-06/27.

[4] *BABAR* Collaboration, B. Aubert *et al.*, BABAR-CONF-06/39.

[5] Belle Collaboration, H. Ishino *et al.*, Phys. Rev. Lett. **95**, 101801 (2005);
Belle Collaboration, K. Abe *et al.*, Phys. Rev. Lett. **94**, 181803 (2005);
Belle Collaboration, Y. Chao *et al.*, Phys. Rev. D **69**, 111102 (2004).

[6] *BABAR* Collaboration, B. Aubert *et al.*, BABAR-CONF-06/37.

[7] Belle Collaboration, A Gordon *et al.*, Phys. Lett. B **542** 183 (2002).

[8] A. Bevan, Mod. Phys. Lett. **A 21**, No. 4, 305 (2006).

[9] *BABAR* Collaboration, B. Aubert *et al.*, Phys. Rev. Lett. **95**, 041805 (2005);
BABAR Collaboration, B. Aubert *et al.*, Phys. Rev. Lett. **93**, 231801 (2004).

[10] G. Kramer and W. Palmer, Phys. Rev. D **45**, 193 (1992);
D. Ebert *et al.*, Phys. Rev. D **56**, 312 (1997);
A. Ali *et al.*, Phys. Rev. D **58**, 094009 (1998);
Y.-H. Chen *et al.*, Phys. Rev. D **60**, 094014 (1999);
H.-Y. Cheng and K.-C. Yang, Phys. Lett. B **511**, 40 (2001);
M. Suzuki, Phys. Rev. D **66**, 054018 (2002);
Y. Li and C. Lü, Phys. Rev. D **73** 014024 (2006);
C. Lü, hep-ph/0606094.

[11] H. Li and S. Mishima, Phys. Rev. D **73** 114014 (2006).

[12] *BABAR* Collaboration, B. Aubert *et al.*, Nucl. Instr. Methods Phys. Res., Sect. A **479**, 1 (2002).

[13] Geant4 Collaboration, S. Agostinelli *et al.*, Nucl. Instr. Methods Phys. Res., Sect. A **506**, 250 (2003).

[14] S. Eidelman *et al.*, Phys. Lett. B 592, 1 (2004) and 2005 partial update for edition 2006.

[15] *BABAR* Collaboration, B. Aubert *et al.*, Phys. Rev. D **66**, 032003 (2002).

[16] *BABAR* Collaboration, B. Aubert *et al.*, Phys. Rev. Lett. **89**, 281802 (2002).

[17] *BABAR* Collaboration, B. Aubert *et al.*, hep-ex/0603050 (accepted for publication in PRL); Belle Collaboration, K. Abe *et al.*, hep-ex/0507096.

[18] Belle Collaboration, A. Gordon *et al.*, Phys. Lett. B **542**, 183 (2002);
BABAR Collaboration, B. Aubert *et al.*, Phys. Rev. Lett. **91**, 201802 (2003);
BABAR Collaboration, B. Aubert *et al.*, Phys. Rev. Lett. **93**, 051802 (2004);
Belle Collaboration, J. Zhang *et al.*, Phys. Rev. Lett. **94**, 031801 (2005).

[19] *BABAR* Collaboration, B. Aubert *et al.*, hep-ex/0605024 (accepted for publication in PRD-RC).

[20] E. Barberio *et al.*, hep-ex/0603003 and online update at `http://www.slac.stanford.edu/xorg/hfag`.

[21] The phase-space-motivated distribution used to parameterise the m_{ES} distribution for $q\overline{q}$ and $b \rightarrow c$ backgrounds takes the form:
$A(m\,; m_0, \xi) = \frac{1}{N} \cdot m\sqrt{1-(m/m_0)^2} \cdot \exp(\xi\,(1-(m/m_0)^2)) \cdot \theta(m < m_0)$,
where $\theta(m < m_0) = 1$ and $\theta(m > m_0) = 0$.

[22] The definition used for a Gaussian with exponential tail is given by
$CB(m\,; m_0, \sigma, \alpha, n) = \frac{1}{N} \cdot \exp\left(-(m-m_0)^2/(2\sigma^2)\right),\ m > m_0 - \alpha\sigma$
and $\frac{1}{N} \cdot \dfrac{(n/\alpha)^n\ \exp(-\alpha^2/2)}{((m_0-m)/\sigma + n/\alpha - \alpha)^n},\ m \leq m_0 - \alpha\sigma$.

[23] O. Long *et al.*, Phys. Rev. D **68**, 034010 (2003).

[24] M. Gronau, D. London, Phys. Rev. Lett. **65**, 3381 (1990).

[25] Belle Collaboration, A. Somov *et al.*, Phys. Rev. Lett. **96** 171801 (2006).

[26] A. Falk *et al.*, Phys. Rev. D **69**, 011502 (2004).

[27] G. Feldman and R. Cousins, Phys. Rev. D **57**, 3873 (1998).

[28] J. Charles *et al.*, Eur. Phys. Jour. C **41**, 1-131 (2005).

[29] M. Bona *et al.*, JHEP **080** 0603 (2006).

[30] M. Beneke *et al.*, Phys. Lett. B **638** 68-73 (2006).

[31] *BABAR* Collaboration, B. Aubert *et al.*, hep-ex/0607057;
Belle Collaboration, J. Zhang *et al.*, Phys. Rev. Lett. **95** 141801 (2005).